doi:10.1093/brain/awn362 Brain 2009: 132; 635–644 | 635

BRAIN
A JOURNAL OF NEUROLOGY

Retinotopically defined primary visual cortex in Williams syndrome

Rosanna K. Olsen,[1] J. Shane Kippenhan,[1] Shruti Japee,[1] Philip Kohn,[1] Carolyn B. Mervis,[2] Ziad S. Saad,[3] Colleen A. Morris,[4] Andreas Meyer-Lindenberg[1,*] and Karen Faith Berman[1]

1 Section on Integrative Neuroimaging, Clinical Brain Disorders Branch, National Institute of Mental Health, NIH, DHHS, Bethesda, MD, USA
2 Department of Psychological and Brain Sciences, University of Louisville, Louisville, KY, USA
3 Scientific and Statistical Computing Core, National Institute of Mental Health, Bethesda, MD, USA
4 Department of Paediatrics, University of Nevada School of Medicine, Las Vegas, NV, USA

*Present address: Central Institute of Mental Health, Mannheim, Germany.

Correspondence to: Karen F. Berman,
10 Centre Drive, Rm 4C101, Bethesda,
MD 20892-1365, USA
E-mail: karen.berman@nih.gov

Williams syndrome, caused by a hemizygous microdeletion on chromosome 7q11.23, is characterized by severe impairment in visuospatial construction. To examine potential contributions of early visual processing to this cognitive problem, we functionally mapped the size and neuroanatomical variability of primary visual cortex (V1) in high-functioning adults with Williams syndrome and age- and IQ-matched control participants from the general population by using fMRI-based retinotopic mapping and cortical surface models generated from high-resolution structural MRI. Visual stimulation, consisting of rotating hemicircles and expanding rings, was used to retinotopically define early visual processing areas. V1 boundaries based on computed phase and field sign maps were used to calculate the functional area of V1. Neuroanatomical variability was assessed by computing overlap maps of V1 location for each group on standardized cortical surfaces, and non-parametric permutation test methods were used for statistical inference. V1 did not differ in size between groups, although its anatomical boundaries were more variable in the group with Williams syndrome. V1 overlap maps showed that the average centres of gravity for the two groups were similarly located near the fundus of the calcarine fissure, ~25 mm away from the most posterior aspect of the occipital lobe. In summary, our functional definition of V1 size and location indicates that recruitment of primary visual cortex is grossly normal in Williams syndrome, consistent with the notion that neural abnormalities underlying visuospatial construction arise at later stages in the visual processing hierarchy.

Keywords: Williams syndrome; retinotopy; V1; primary visual cortex; visuospatial construction

Introduction

Williams syndrome, a neurodevelopmental condition caused by hemizygous deletion of approximately 25 genes on chromosome 7q11.23, is characterized by mild-to-moderate intellectual disability, relatively preserved language and verbal short-term memory abilities and marked visuospatial construction deficits (Meyer-Lindenberg *et al*., 2006). This pattern of cognitive strengths and weaknesses has been operationalized into a highly specific and sensitive 'Williams syndrome cognitive profile'

Received May 16, 2008. Revised December 2, 2008. Accepted December 4, 2008

(Mervis *et al*., 2000). The syndrome is of particular interest because it represents a rare case in which an established human genetic mechanism can be related to a remarkably specific cognitive phenotype and the neural substrate explored with structural and functional neuroimaging.

Behavioural studies have focused on dissociating relative strengths and weaknesses in visual processing with the aim of providing clues about brain areas affected by Williams syndrome. The hallmark cognitive deficit of the disorder, visuospatial construction, is manifested by poor performance on tasks that depend on 'the ability of an individual to see an object in terms of a set of parts and use those parts to construct a replica of the pictured object' (Frangiskakis *et al*., 1996). It is traditionally tested by assembling blocks into a prescribed design and depends upon cognitive operations that fall largely in the visuospatial construction domain (Bellugi *et al*., 1988, 1994; Mervis *et al*., 1999; Morris and Mervis, 1999, 2007), thus implicating dorsal visual processing areas as defined by Ungerleider and Mishkin (1982) in monkeys and Haxby *et al*. (1991) in humans. A number of studies have provided behavioural evidence of impaired visuospatial cognition specifically associated with dorsal stream function but relatively unimpaired performance on visual tasks associated with ventral stream function for individuals with Williams syndrome (Atkinson *et al*., 1997, 2003; Bellugi *et al*., 2000; Paul *et al*., 2002; Farran, 2006; Landau *et al*., 2006; Vicari and Carlesimo, 2006).

In particular, individuals with Williams syndrome perform at about the same level as mental-age matched typically developing individuals on tasks associated with ventral stream function (e.g. form coherence, indicating which picture matched the orientation of a mail slot, object recognition, memory for objects) but at a significantly lower level on tasks associated with dorsal stream function (e.g. perception of form from motion, accuracy in inserting a card in a mail slot at various orientations, memory for object location).

The fact that performance on object-oriented tasks is relatively unimpaired for individuals with Williams syndrome suggests that early visual areas, which are necessary to support these hierarchically more advanced ventral stream processes, are functionally intact (Atkinson *et al*., 1997; Bellugi *et al*., 1999, 2000). Indeed, performance on tests of visual acuity, stereopsis and visual field does not account for the impairments on visuospatial construction tasks (Atkinson *et al*., 2001), providing further support for unimpaired early visual processing neural centres. In addition, global motion studies, in which participants with Williams syndrome have demonstrated a specific deficit, do not differentially activate V1 (Braddick *et al*., 2000). A recent study which examined *in vivo* retinal thickness, optic disk concavity and psychophysical measures of visual performance found that individuals with Williams syndrome had a significantly reduced retinal thickness, with the magnocellular pathway particularly affected. Interestingly, retinal thickness was correlated with low-level motion detection task performance but not with higher-level visuospatial processing tasks (Castelo-Branco *et al*., 2007). While the findings of some studies of brain structure have suggested that early visual areas may be altered in Williams syndrome (Reiss *et al*., 2000, 2004; Schmitt *et al*., 2001; Galaburda *et al*., 2002; Van Essen *et al*., 2006), others have not found structural macroanatomical abnormalities in this region (Meyer-Lindenberg *et al*., 2004; Eckert *et al*., 2006).

Given these conflicting data, in the present study, we sought to establish the neurofunctional status of early visual processing in Williams syndrome. We used standard fMRI-based retinotopic mapping procedures (Engel *et al*., 1994; Sereno *et al*., 1995; DeYoe *et al*., 1996) to directly and specifically probe primary visual cortex, or V1, the earliest cortical visual area, by measuring each individual's functionally defined V1 surface area. Next, we investigated between-group differences in V1's spatially normalized anatomical locale and its variability. Since individuals with Williams syndrome often have mild-to-moderate intellectual disability, neuroimaging studies of this population are faced with particular challenges regarding participant compliance and control group selection. Regarding the latter, comparing a group of low-IQ Williams syndrome participants to a group of normal-IQ controls would represent a potential confound that would impact on the interpretation of the neuroimaging data because group differences could be attributable to differences in intellectual ability *per se*, rather than to conditions specific to Williams syndrome. To avoid these issues, we recruited an exceptional group of participants with Williams syndrome with normal intelligence. This exceptional Williams syndrome cohort was not only able to cooperate with the complexities and demands inherent in retinotopic mapping, but also allowed us to select an IQ-matched comparison group composed of individuals from the general population. We took this approach (i) because abnormalities found even in this high-performing group are likely to be characteristic of this syndrome as a whole, (ii) because of the exacting level of cooperation and attention required for technically adequate retinotopic mapping and (iii) because the neurobiological phenotype will be close to the genetic substrate of the disorder, consistent with our overall objective of using neuroimaging to forge a link between the effects of specific genes and brain mechanisms of cognitive and behavioural disorders. Our participants with Williams syndrome were, therefore, matched with healthy controls not only for age and handedness, but for IQ as well (Table 1), and they were also in good physical health.

Methods

Participants

Ten participants with Williams syndrome (5F, 5M; Mean age = 31.3 years; SD = 9.0) with normal IQ (Mean = 92.1, SD = 8.8) and 10 demographically matched (3F, 7M; Mean age = 29.3 years; SD = 5.0; mean IQ = 96.2, SD = 7.4) controls from the general population completed this study (Table 1). Participants with Williams syndrome were genetically tested with fluorescent *in situ* hybridization (FISH) to verify the Williams syndrome diagnosis and define the extent of the deletion; all participants with Williams syndrome had classic hemideletions on chromosome 7q11.23. IQs were measured by the two-subset form of

Table 1 Participant demographics

	Gender	Age	Handedness	IQ
Controls	3F, 7M	29.3 years	100% right	96.2
Williams syndrome	5F, 5M	31.3 years	100% right	92.1
P-value	0.361	0.545		0.274

the Wechsler Abbreviated Scale of Intelligence (Wechsler, 1999) for participants with Williams syndrome and a short form of the Wechsler Adult Intelligence Scale-Revised (Wechsler, 1981) for controls. These participants, despite having overall IQs in the low-normal to normal range, demonstrate the classic visuospatial construction deficit that typifies the syndrome. The *T*-score of this group on the Block Design test (a neuropsychometric test that is used to assess visuospatial construction impairment in this and other patient populations) was almost 1.5 standard deviations below that of the general population [35.4 ± (SD) 7.3 versus 50 ± 10]. Control participants were screened for medical and psychiatric conditions and for drug or alcohol abuse. All participants provided written informed consent as specified by the National Institute of Mental Health Internal Review Board.

Scanning procedures

Functional and structural scanning parameters

Participants completed five runs of functional MRI scanning (GE EPI sequence; 18 coronal slices; 4-mm thick, in-plane resolution of 3.75 × 3.75 mm; TR:2000 ms; TE:30; 160 reps). fMRI scanning was conducted with a 1.5T scanner (GE Signa, Milwaukee, WI) using a standard bird-cage head coil. For surface extraction and modelling, six high-resolution structural images (SPGR sequence, 124 slices, TE = 5.2 ms, TR = 12ms, FOV = 24 mm, resolution 0.9375 × 0.9375 × 1.2 mm) were collected for each participant on a 1.5T scanner (GE Signa).

Task design

Following standard retinotopic mapping procedures (Engel *et al*., 1994; Sereno *et al*., 1995; DeYoe *et al*., 1996), two types of visual stimuli were used to map polar angle and eccentricity: (i) black and white rotating checkerboard hemifield (rotating period = 40 s) and (ii) expanding ring stimuli on a black background (visual angle = 18°; flicker frequency = 8 Hz; expanding period = 32 s). Previous studies have shown attentional effects on BOLD response in primary visual cortex (Watanabe and Shimojo, 1998; Brefczynski and DeYoe, 1999; Kastner *et al*., 1999; Somers *et al*., 1999); therefore, a simple button-press task was employed to engage the participants and also to ensure fixation to the centre of the screen throughout the trial. In the rotating checkerboard task, participants were instructed to decide whether a coloured line superimposed on the central fixation point was red or blue and make a button press accordingly. The target line appeared for 100 ms at intervals that varied randomly between 4.5 and 5 s. In the expanding ring task, participants pressed the button each time they detected the onset of a new ring expansion from the centre. Stimuli were presented through a binocular fibre-optic goggle system (Avotec model SS-3100), and participants' eyes were continuously monitored with a camera to ensure fixation.

Image processing

Structural images were intensity normalized, registered and averaged to improve signal to noise. The averaged image was then registered, using AFNI's (Cox, 1996) '3dvolreg' tool (with 6 DF), to an additional structural image acquired just prior to the first functional image run. FMRIB's 'Brain Extraction Tool' [BET, (Smith, 2002)] was used in combination with MEDx's 'Interactive Segmentation' (Medical Numerics, Inc., Sterling, Virginia) to remove extracranial matter. Freesurfer ver. 0.9 (Dale *et al*., 1999; Fischl *et al*., 1999*a*) was used to segment grey and white matter and create white matter and pial surface representations for each participant. These surface representations consisted of large numbers of points, or nodes, typically 150 000, connected in a triangular mesh.

Functional data were visually checked for artifacts and movement-related spikes. Participants were excluded from further analysis, if any within-run movement parameters exceeded 2 mm. Based on these criteria, data from four of 14 participants with Williams syndrome and two of 12 control participants were excluded. Functional data that survived these stages were then subjected to further pre-processing, using several AFNI tools. Within each run, slice time acquisition correction was performed to account for interleaved acquisition, after which each functional run was volume registered to the first volume acquired in the series. Images were spatially smoothed with a 2 mm FWHM Gaussian kernel and then averaged to increase the signal-to-noise ratio in the functional dataset (using '3dTshift', '3dvolreg', '3dmerge' and '3dMean', respectively). Using FMRIB's 'Linear Image Registration Tool' [FLIRT (Jenkinson *et al*., 2002)], each participant's functional datasets were registered to the high-resolution structural image from which the surface representation was created. This automated registration was subjected to visual inspection and manual adjustments, using the Freesurfer tool 'tkregister2' as well as SPM's 'Check Registration' tool (Friston *et al*., 1995). Additionally, AFNI's '3ddelay' tool was used to compute maps of response delays relative to ideal waveforms based on the retinotopic stimuli.

Analysis of V1 regions

Specific image analysis tools were chosen to allow us to address questions regarding size and localization of early visual areas. The first question was whether there were group differences in surface area of functionally defined V1. Two additional questions addressed the normalized anatomical locus of the V1 region: (i) is the anatomical variability of V1 within one group greater than the other? and (ii) are there between-group differences in V1 locations when compared in a normalized surface space?

Functional definition of V1 surface area and hemispheric area

We used Freesurfer tools to compute a region of interest (ROI) within each hemisphere of each participant that contained the portion of V1 that represented the visual field from 2 to 16° of eccentricity using the following procedures. First, a Fourier analysis of the two functional datasets for each individual produced maps of polar angle (which is mapped onto visual cortex with the rotating-wedge stimuli) and eccentricity (from the expanding-ring stimuli). From these results, field sign maps, which indicate whether the retinotopically organized visual field representations are mirror-reversed or preserved in cortex, were calculated and then displayed on the inflated surface (Fig. 1). The cortical area that contains the foveal representation is shared by multiple early visual areas; thus, we excluded the central 2° from the ROIs as indicated by the eccentricity phase maps (Dougherty *et al*., 2003). Using the field sign maps to define superior and inferior borders, and corresponding eccentricity maps to define anterior and posterior extent, V1–V2 borders were manually traced to produce a V1 ROI on each participant's native space surface model, as illustrated in Fig. 2. In-house tools were developed to visualize the 2° and 16° eccentricity locations and these were used to draw the posterior and anterior boundary lines of V1. Eccentricity maps from 3ddelay were used to aid and confirm the mapping of surface values to visual angles. This tracing was performed using SUMA ROI drawing tools (Saad *et al*., 2006) while blind to participant identity and diagnosis.

Two analyses were carried out to account for the smaller brain size that has been reported in Williams syndrome (Reiss *et al*., 2000).

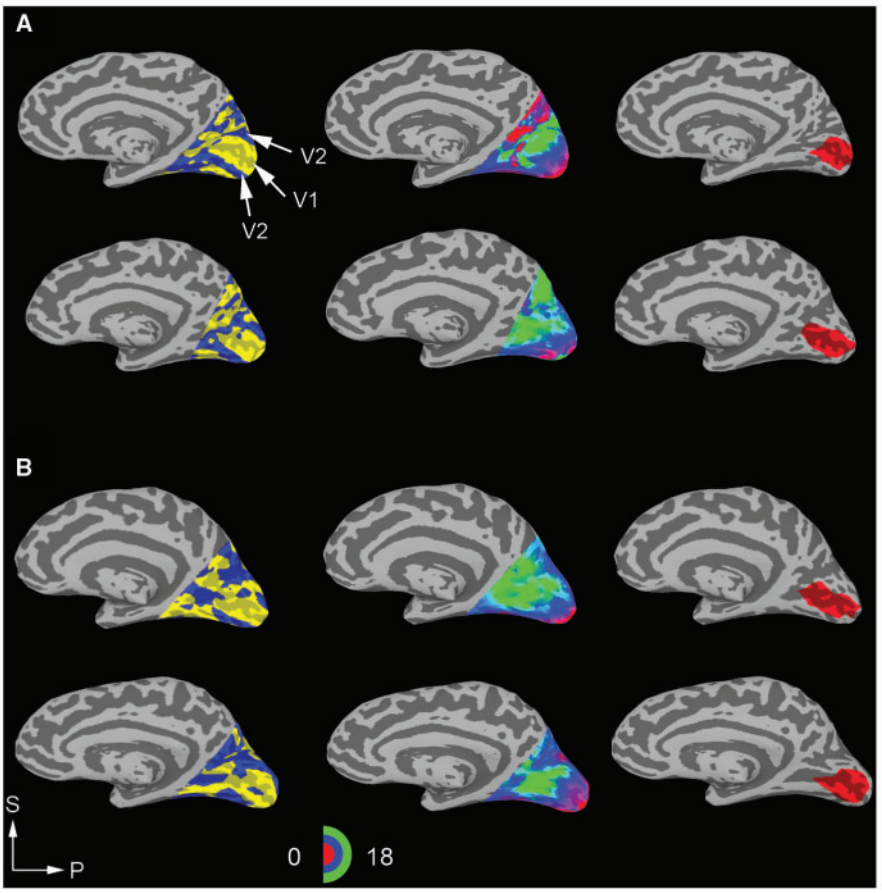

Figure 1 Left panel: Representative examples of field sign maps for two control participants (**A**) and two participants with Williams syndrome (**B**) displayed on each participant's own inflated cortical surface representation. Yellow indicates mirror-image-mapped areas; blue indicates non-mirror-image areas. V1 and V2 labels indicate corresponding regions in the retinotopic map. Centre panel: Right hemisphere eccentricity maps. Red colours indicate regions corresponding to the centre of the field of view, while green regions correspond to the outer eccentric degrees (see colour bar). Right panel: V1 ROIs displayed in red on the participants' own cortical surface representation. Note the good correspondence between the V1 ROI and the calcarine fissure, as well as the high variability of the anatomy of the calcarine fissure itself. The axes labelled S (Superior) and P (Posterior) provide anatomical orientation.

First, Freesurfer's *mris_anatomical_stats* tool was used to compute statistics for whole hemispheres and for the specified V1 regions. The surface areas for each V1 ROI as well as the total hemispheric surface areas were computed on the white matter surface (Fischl *et al*., 1999b). Second, an operator who was blind to subject identity manually delineated the medial aspect of the occipital lobe of each participant's cortical surface. The parieto-occipital sulcus served as the anterior border of this roughly triangular portion of the occipital surface. The superior and inferior borders were defined by the intersection of the medial aspect with the superior and inferior aspects of the occipital lobe, respectively. We computed V1 to medial occipital lobe ratios and submitted these ratios to our statistical analysis. Data were analyzed using ANOVA as implemented in Statistica (Statsoft, Tulsa, OK), with hemisphere as a within-subject (repeated measures) factor and diagnosis as a categorical predictor (between-groups random-effects) factor. This analysis was performed on whole hemisphere surface areas, on absolute V1 surface area values and on values computed both as a ratio of V1 area to total hemispheric area and as a ratio of V1 area to medial occipital lobe area.

Anatomical locale of V1 and its variability

The individual V1 ROIs described above were then projected to a standardized average cortical surface, based on a spherical surface-based registration (Fischl *et al*., 1999*b*), to compare the spatial distributions of V1 between individuals and between groups in a standardized space. To avoid any potential bias in the spherical registration, a customized template using all participants from both groups was first created with Freesurfer's *mris_make_template* tool. Next, the normalized V1 ROIs within each group were overlaid, and a node-by-node summation was performed to construct a surface-based 'overlap map', or 'probability map' (Amunts *et al*., 2000; Wohlschlager *et al*., 2005), in which the value assigned to each node (specified by a particular displayed colour value) designated the percentage of participants within a group whose V1 area contained that node (Fig. 3A). For example, if all 10 of the V1 ROIs for a particular group (Williams syndrome or control) were represented in a given node, that node was colour-coded in red, while if a given node intersected with only 1 out of the 10 participants' V1s, that node was colour-coded in blue.

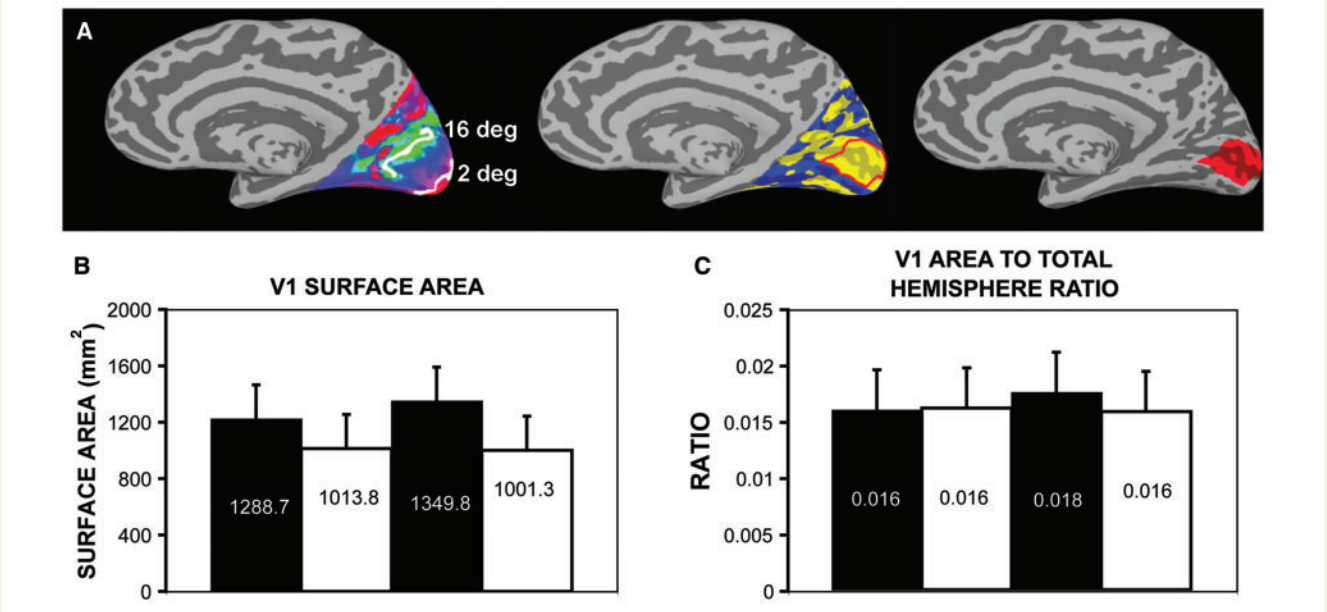

Figure 2 (**A**) Retinotopic mapping procedure used to define each participant's V1 ROI. Left, one participant's eccentricity map, white lines demarcate the 2 and 16° eccentricities. V1/V2 boundaries are drawn on the field sign map (centre image), and the posterior (2°) and anterior extent (16°) were defined with the eccentricity map. Right, the completed ROI for this example subject. (**B**) Mean absolute surface area (measured in mm^2) for controls and participants with Williams syndrome. (**C**) Means of values corresponding to the ratio of V1 surface area to total hemisphere surface area. See text for ANOVA results.

Each of the separate colour levels delineated a region of cortical surface within which a particular percentage of participants' functionally defined V1 overlapped. The surface area for each group was plotted with respect to the number of overlapping participants, to assess whether the within-group anatomical variability of the functionally defined V1 region differed between the two groups (Fig. 3B). We reasoned that if we found relatively large surface areas which corresponded to low participant overlap, this would imply low coincidence of V1 representations (more variability in V1 locale), while relatively large surface areas corresponding to high participant overlap would imply more anatomical consistency of V1 locales within that group. We tested for between-group differences in these distributions using a non-parametric (Kolmogorov–Smirnov) test, which is generally regarded as one of the most useful and general non-parametric methods for comparing two samples, and is sensitive to differences in both location and shape of the empirical cumulative distribution functions of two samples (Brunk, 1965).

In addition, we performed permutation tests to determine whether the overlap maps on the cortical surface differed between the two groups, based on the centres of gravity within the overlap maps. The distance (in mm) between the two groups' centres of gravity was computed and this distance was used as the statistic of interest. Statistical testing consisted of randomly permuting the members of the two groups 1000 times, and recording this statistic. The *P*-value for this test corresponded to the rank position of the statistic in the canonical case (the correct labelling of the Williams syndrome and control group) in the distribution of that statistic generated from all 1000 permutations. The null hypothesis (i.e. that the two groups have the same centre of gravity) was rejected only if the permuted distance exceeded the canonical distance fewer than 50 out of 1000 times (corresponding to $P<0.05$).

To rule out the possibility that any differences identified with these tests was an artefact of the spherical normalization process, curvature maps (displaying sulcal patterns) for each participant were projected onto the normalized average surface. Group averages of these curvature maps were then visualized to ensure that the calcarine fissure was in good alignment with the spherical template for both groups (see Supplementary Fig. S1).

Results

Behaviour

Both groups responded to the attentional task with a high degree of accuracy—participants responded correctly to the target stimuli with a button press during >90% of the trials, demonstrating good central fixation. Technical difficulties prevented the collection of behavioural data for four of the 10 Williams syndrome participants. The mean IQ of these participants (92) was identical to that of the remaining six Williams syndrome participants. In all cases, fixation was observed via a camera throughout scanning.

Functionally defined V1 surface area and total hemisphere area

Consistent with previous reports of smaller brain size in Williams syndrome, the two-way ANOVA showed a main effect of group on whole-brain surface area [$F(1,18)=10.541$, $P=0.004$]. Neither the main effect of hemisphere [$F(1,18)=3.187$, $P=0.091$] nor the group by hemisphere interaction [$F(1,18)=2.601$, $P=0.124$] was significant. With regard to the area of V1, itself, a significant difference in the between-group comparison of *absolute* V1 area was noted [$F(1,18)=5.86$ $P=0.026$]. For absolute V1 areas,

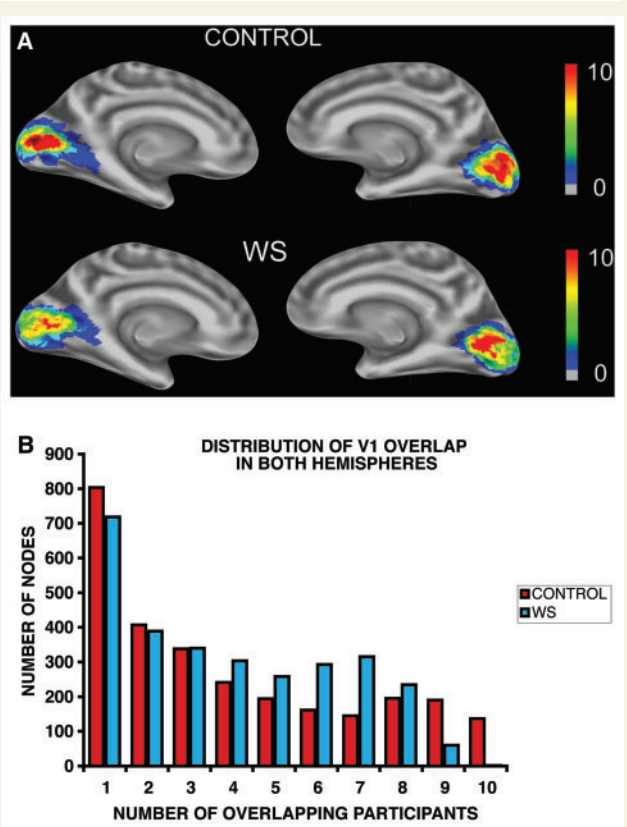

Figure 3 (**A**) Maps of V1 overlap on a standardized cortical surface for controls and participants with Williams syndrome, demonstrating a non-significant trend toward an anterior/ventral shift in measured V1 locale for participants with Williams syndrome. Warm colours show greater percentage of participant overlap (up to a maximum number of 10/10 participants), while cool colours show less overlap (down to a minimum of 1/10 participants). Top panel: V1 overlap in controls, left and right hemispheres. Bottom panel: V1 overlap in participants with Williams syndrome, left and right hemispheres. (**B**) Distributions of V1 surface area overlap within each group (collapsed across hemispheres) illustrating the degree to which V1 areas were anatomically coincident within the two groups. Bars indicate the number of nodes occupied in common by 1–10 individuals in each group, respectively. Large surface area (increased number of nodes) for low participant counts (low percentage of the maximum number of participants) imply V1 areas with sparse coincidence (i.e. less overlap) across participants, while large surface area for higher participant counts (higher percentage of maximum) imply more highly coincident V1 topography. A Kolmogorov–Smirnov test indicated a significant difference ($P < 0.001$) between these two distributions.

neither the main effect of hemisphere [$F(1,18) = 0.739$, $P = 0.401$] nor the group by hemisphere interaction [$F(1,18) = 1.097$, $P = 0.309$] was significant.

Crucially, when V1 was considered as a *ratio* to total hemispheric area, a two-way ANOVA demonstrated no significant main effect of group [$F(1,18) = 0.228$, $P = 0.639$], or hemisphere [$F(1,18) = 0.392$, $P = 0.539$] and no group-by-hemisphere interaction [$F(1,18) = 0.861$, $P = 0.366$]. Similarly, when V1 was considered as a ratio using the area of the medial occipital lobe as the denominator, we found no significant main effect of group [$F(1,18) = 2.625$, $P = 0.123$], or hemisphere [$F(1,18) = 0.097$, $P = 0.759$], and no group-by-hemisphere interaction [$F(1,18) = 0.008$, $P = 0.930$]. The results for data normalized by both total hemispheric area and medial occipital lobe area clearly show that the significant difference in absolute V1 area was explained by the overall difference in brain size (Fig. 2).

For both groups, IQ did not correlate significantly with whole-hemisphere surface area (controls: $r = -0.108$, $P = 0.766$; participants with Williams syndrome: $r = -0.423$, $P = 0.224$) or with V1 surface area (controls: $r = -0.324$, $P = 0.361$; participants with Williams syndrome: $r = 0.172$, $P = 0.634$). In the Williams syndrome group, there was no correlation between V1 area and performance on a visuospatial construction task ($r = 0.195$, $P = 0.589$), which the participants completed in a separate scanning session (Meyer-Lindenberg *et al*., 2004).

Anatomical locale of V1 and its variability

As expected, the overlap maps (Fig. 3) showed approximate uniformity in the location of V1 for both participants with Williams syndrome and control participants. However, from these overlap maps it was qualitatively apparent that the control group's V1s were more consistent in neuroanatomical locale as demonstrated by more red areas in the controls' overlap maps and more yellow and green areas in the Williams syndrome overlap maps. The distributions shown in Fig. 3B display and quantify this observation, as the number of nodes with only 4–8 overlapping V1s was much greater for the Williams syndrome group, while the number of nodes where 9–10 V1s overlapped was much greater in controls. A Kolmogorov–Smirnov test comparing these distributions demonstrated significant between-group differences ($P < 0.001$) in V1 anatomical variability across both hemispheres. Thus, this result was due to a different pattern of overlap distribution in Williams syndrome: the amount of V1 surface area occupied in common by a high percentage of participants with Williams syndrome was small compared to controls, whereas the amount of surface area occupied by only a few Williams syndrome V1s was relatively large compared with controls, both indicating that Williams syndrome V1 spatial locale is less consistent than in control participants. We also performed this analysis for each hemisphere separately (left hemisphere: $P = 0.0008$; right hemisphere: $P = 0.0011$).

By inspection of the overlap maps (Fig. 3A), V1s appeared to be localized slightly more anteriorly and ventrally within the occipital cortex of participants with Williams syndrome than in control participants. In the left hemisphere, the location of greatest within-group V1 overlap or 'centre of gravity' in controls was located ~24.5 mm away from the occipital pole, while the centre of gravity in Williams syndrome participants was 27.0 mm away from the pole (Fig. 4). Similarly, in the right hemisphere, the centre of gravity in controls was located more posteriorly (21.8 mm away from the pole) than the centre of gravity in Williams syndrome (24.6 mm away from the pole; see Fig. 4). Importantly, MNI

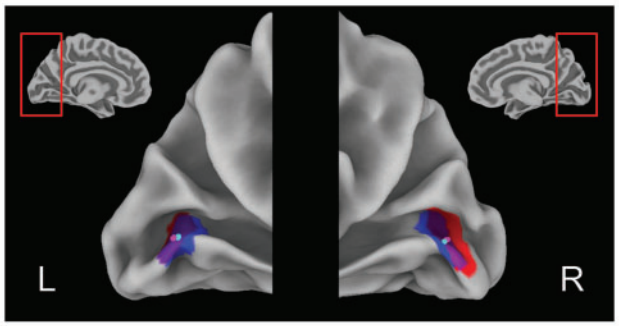

Figure 4 Nodes containing the V1 centres of gravity for each group in the left and right hemispheres of the average (across all participants) surface rendering. The cyan and pink dots represent the centres of gravity of V1 regions for the Williams syndrome and control groups, respectively. The distance between each participant's V1 centre of gravity and the group's centre of gravity was computed. The standard errors for Williams syndrome (blue) and for controls (red) are displayed on the left and right surface. Regions of standard error overlap are shown in purple. Centres of gravity are located in the calcarine fissure for both groups, but are slightly more anterior and ventral in the Williams syndrome group.

coordinates for the V1 centre of gravity in controls (LH: −8, −79, 4; RH: 11, −81, 4) and Williams syndrome (LH 6, −77, 5; RH: 7, −78.4) were located in similar positions as previously reported in the literature (Hasnain *et al*., 1998; Wohlschlager *et al*., 2005).

In Fig. 4, the centre of gravity and its associated standard error for each group are displayed on a normalized average surface. The cyan and pink dots represent the centres of gravity of V1 regions for the Williams syndrome and control groups, respectively. The red and blue regions represent the areas within a radius (on the spherical surface) corresponding to the standard error of these individual distances from the group centre of gravity. Distances from the group centres of gravity to the centres of gravity of each of the individuals within the group were computed on spherical surfaces. While these subtle differences in the location of the centre of gravity were noted on inspection of the overlap difference maps and centre of gravity coordinates, permutation tests found no significant between-group differences in this parameter in either hemisphere (left hemisphere, $P = 0.406$; right hemisphere, $P = 0.076$).

Discussion

Our work provides the first use of retinotopy to define the functional neuroanatomy of V1 in Williams syndrome and one of the first uses of this technique in a human pathological condition that affects visuospatial processing. Surface-based methodology (Van Essen, 2004) was essential in delineating both the cortical extent of V1 and its spatial location relative to anatomical landmarks such as the occipital pole and the calcarine fissure, and creating overlap maps for each group (Amunts *et al*., 2000; Wohlschlager *et al*., 2005) was crucial for examining anatomical variability. With regard to spatial extent, the functionally defined V1 surface area was unaltered in Williams syndrome. In addition, our previous study of functional activation of the dorsal and ventral visual processing streams in Williams syndrome (Meyer-Lindenberg *et al*., 2004), while not specifically designed to probe early visual processing, did not find abnormalities in V1, but, rather demonstrated functional and structural abnormalities in hierarchically later dorsal stream areas. Taken together, these findings are consistent with and help to define the neurobiological basis of the behavioural data for individuals with Williams syndrome that indicate (i) intact early visual processing, (ii) relatively spared ventral stream cognitive operations and (iii) impairment on visuospatial tasks related to the dorsal stream (Atkinson *et al*., 1997; Bellugi *et al*., 2000; Paul *et al*., 2002; Landau *et al*., 2006; Vicari and Carlesimo, 2006; Mervis and Morris, 2007).

While the present study focused on the functional definition of the boundaries and spatial extent of V1 proper, several investigations of the anatomy of the occipital lobe as a whole in Williams syndrome have been reported. Some of these have defined brain shape differences in Williams syndrome based on anatomical MRIs (Schmitt *et al*., 2001; Reiss *et al*., 2004). These studies used shape-based morphological analysis, ROI methods and voxel-based morphometry; they report smaller Williams syndrome brains, smaller occipital cortices and decreases in cortical and subcortical extrastriate areas. Our study's findings, in part, complement those of Reiss *et al*. (2004) and Thompson *et al*. (2005); we found decreased hemispheric areas and noted a tendency for V1 to be smaller in Williams syndrome, but only when V1 area was not corrected for the between-group difference in overall brain size. In a voxel-based morphometry analysis of a group of participants with Williams syndrome that included the individuals in the present study, we did not find any grey or white matter changes in the region around the calcarine sulcus (Meyer-Lindenberg *et al*., 2004).

Our V1 measurements in control participants align well with those from previously published reports using similar retinotopic mapping procedures (Dougherty *et al*., 2003; Wohlschlager *et al*., 2005) as well as with histological studies of Brodmann Area 17 (Amunts *et al*., 2000). In the present study, we measured a subregion of V1 representing 2–16° of the visual field. Dougherty and colleagues used a slightly smaller visual angle, reporting V1 measurements representing 2–12°. Nevertheless, the mean surface area measurements from the control participants in this study (mean V1 measurement: 1286.3 mm^2) are very similar to those of Dougherty and colleagues (mean V1 measurement: 1470 mm^2). Conner *et al*. also measured V1 in adults from the general population and reported a comparable, albeit slightly smaller, size of V1 (800–1200 mm^2) using eccentricity stimuli that extended 15° on the diagonal (Conner *et al*., 2004). Further, our results replicate those of Hasnain and colleagues who reported highly similar MNI coordinates for V1 centre for gravity (Hasnain *et al*., 1998).

The cellular properties of V1 in postmortem Williams syndrome brains have been explored by Galaburda *et al*. (2002); that study reported cell-packing density differences as well as cell size differences, in the left hemisphere only, with interactions between cell-packing density and layers in peripheral visual cortex (Galaburda *et al*., 2002). However, the functional implications of these findings are unclear because individuals with Williams syndrome do

not show early visual processing deficits *per se*. Our study suggests that the histological findings do not translate into reduced V1 surface area as defined functionally by retinotopy *in vivo*.

Visualization of the V1 overlap maps revealed anatomical variability within and between groups. Our formal statistical analysis of localization of V1 using surface-based overlap maps showed significantly more between-participant anatomical variability in Williams syndrome and but no significant differences in V1 centre of gravity between the Williams syndrome and control groups. This is particularly intriguing in light of our previous findings of statistically decreased grey matter volume (and decreased sulcal depth) in the region of the intraparietal sulcus in this participant population (Meyer-Lindenberg *et al*., 2004; Kippenhan *et al*., 2005), since it is conceivable that the intraparietal structural change might be accompanied by variability in locale in other visual areas, such as that seen in Figs 3 and 4 and reflected by other studies (Schmitt *et al*., 2001; Reiss *et al*., 2004). Our results, while not uncovering a significant difference in locale on the group level, provide a cautionary note for histopathological studies of this region and others in individuals with Williams syndrome because typical neuroanatomical landmarks may not correspond to architectonic characteristics. For example, if V1 were located more ventrally in some individuals with Williams syndrome, the dorsal bank of the calcarine sulcus in those individuals could contain neurons that are functionally and architectonically part of V2, a region that normally corresponds to BA18, which may have higher cell density than BA 17 (Brodmann, 1909; Amunts *et al*., 2000). This speculation further demonstrates the importance of *in vivo* delineation of the extent and locale of functionally recruited cortical regions in genetically determined pathological conditions such as Williams syndrome.

Several caveats and remaining questions should guide future studies in this area. First, as retinotopic mapping utilizes different experimental procedures and analysis techniques than more traditional activation studies, our findings do not immediately translate to other paradigms used to assess V1 activity, such as those that compare a more active state to a low-level baseline task. fMRI studies of face and gaze processing and global image processing abilities of individuals with Williams syndrome did in fact report evidence of abnormal early visual stream dysfunction as well as dysfunction in a number of additional areas, but participant selection and methods were quite different from ours (Mobbs *et al*., 2004, 2007) and those experiments were not designed to address the elementary type of visual processing that is the cognitive domain of V1. Furthermore, early visual areas were only included in a large cluster encompassing a number of other regions, and the methodology employed was not optimized for localizing dysfunction in early visual cortex. Further advances in our understanding of the neurobiology of Williams syndrome should build on the present results to specifically probe with high-resolution functional neuroimaging whether normal V1 cortical extent translates into normal V1 function during early visual perception tasks in Williams syndrome. Second, high-field strength diffusion tensor imaging of the visual areas and retinotopic mapping of other occipital areas in individuals with Williams syndrome will also be an important adjunct.

Further, the null findings from this study should be interpreted carefully. While the Williams syndrome cognitive profile would predict that early visual areas would be relatively intact, it is possible that there are very subtle differences in the size and location of V1 that the study did not have the power to detect or that the data for the four subjects who lacked behavioural data contributed to the negative finding. Indeed, while we did find differences in the number of overlapping V1 nodes in Williams syndrome and control participants, indicating more anatomical variability in Williams syndrome, we did not find significant differences when comparing the spatial locale with respect to the centre of gravity. Future studies using more recently developed imaging technology (e.g. surface coils and higher-resolution fMRI sequences) should be used to further explore the retinotopically defined visual areas in Williams syndrome, which will allow the definition of the extent of other cortical areas (V2, V3, VP, etc.).

The compliance and cooperation of our high-functioning participants with Williams syndrome allowed us to demonstrate that the genetics of Williams syndrome do not *mandate* V1 abnormalities, even in individuals who have known dorsal visual steam structural and functional abnormalities [as has been demonstrated in these same participants in Meyer-Lindenberg *et al*. (2004) and Kippenhan *et al*. (2005)] and who demonstrate the hallmark visuospatial abnormality behaviourally. However, it will be important in future studies to also evaluate V1 in intellectually impaired participants to assess the generalizability of our findings to the overall Williams syndrome population. As imaging techniques and facilities improve, such studies may become feasible. Eye-tracking during scanning, which was not employed during the present study, will be an important component of such investigations.

It has been noted that ~50% of the Williams syndrome population has visual problems including strabismus, refractive error and amblyopia (Atkinson *et al*., 2001). In our sample, two participants with Williams syndrome had clinical strabismus, which has been shown to cause functional (stereopsis problems) and microscopic structural (altered horizontal cells in primates and kittens) changes, which, in turn, could lead to higher-level visual problems (Birch and Stager, 1985; Lowel and Singer, 1992; Tychsen *et al*., 2004). However, in a large sample of children with Williams syndrome, Atkinson and colleagues (2001) found no correlation between peripheral visual problems in acuity and stereopsis and the visuospatial construction problems that are paramount in the syndrome. Moreover, even with the inclusion of two participants with Williams syndrome who had strabismus our findings were largely normal.

With respect to our findings on differences in V1 overlap, we specifically addressed potential concerns regarding two crucial aspects of our methodology for which biases or systematic errors could theoretically have produced similar results that were artifactual. These concerns were (i) registration of functional (polar and eccentricity) and structural images and (ii) surface-based spherical registration used to project V1 areas to the standardized surfaces. Regarding the first issue, registrations between functional and structural images were subjected to close visual inspection, using two complementary software visualization tools. The second concern, namely that the spherical registration process had failed to properly align the calcarine fissures of the participants with Williams syndrome with respect to the template, motivated us to create the images in Supplementary Fig. S1, which show patterns of sulcal curvature for both groups. These images clearly demonstrate that the spherical registration of the structural features did not result

in displacement of the calcarine fissures of the participants with Williams syndrome relative to those of the control participants.

In summary, this study provides the first functional brain-imaging evidence that the earliest cortical visual processing area, as measured by retinotopically mapped cortical extent of area V1, is spared in Williams syndrome, a genetic syndrome whose cognitive hallmark is visuospatial construction impairment. This demonstration of largely intact functional neuroanatomy of primary visual cortex in Williams syndrome, together with the lack of correlation between cognitive measures and V1 size, advances our understanding of the neural substrate underlying the genetically based visuospatial construction deficit in Williams syndrome by adding support for the contention that visuospatial processing problems in Williams syndrome are not accounted for by abnormalities in early visual areas (Atkinson *et al*., 1997), but rather emerge from anomalies in later dorsal visual processing stream regions (Meyer-Lindenberg *et al*., 2004, 2006). We also demonstrated an interesting difference in the degree of V1 neuroanatomical variability in Williams syndrome compared with controls, which points to genetic influences in neurodevelopment. This finding should guide future research, specifically the further study of individual genes in the Williams syndrome critical area of chromosome 7q11.23, their actions in the neural development of Williams syndrome, and their role in visual system development in humans.

Supplementary material

Supplementary material is available at *Brain* online.

Acknowledgements

We thank the participants with Williams syndrome and their families, as well as Drs Sean Marrett and Hauke Heekeren for help with MRI scanning and analyses. We also thank Dr Joe Masdeu, Shau-Ming Wei, Joel Bronstein and Angela Ianni for providing image and data processing assistance. Finally, we thank Dr Robert Dougherty for providing consultation on our retinotopic maps.

Funding

DHHS/NIH/NIMH/IRP and NINDS (NS35012 to C.B.M., PI).

References

Amunts K, Malikovic A, Mohlberg H, Schormann T, Zilles K. Brodmann's areas 17 and 18 brought into stereotaxic space-where and how variable? Neuroimage 2000; 11: 66–84.

Atkinson J, Anker S, Braddick O, Nokes L, Mason A, Braddick F. Visual and visuospatial development in young children with Williams syndrome. Dev Med Child Neurol 2001; 43: 330–7.

Atkinson J, Braddick O, Anker S, Curran W, Andrew R, Wattam-Bell J, et al. Neurobiological models of visuospatial cognition in children with Williams syndrome: measures of dorsal-stream and frontal function. Dev Neuropsychol 2003; 23: 139–72.

Atkinson J, King J, Braddick O, Nokes L, Anker S, Braddick F. A specific deficit of dorsal stream function in Williams' syndrome. Neuroreport 1997; 8: 1919–22.

Bellugi U, Lichtenberger L, Jones W, Lai Z, St George MI. The neurocognitive profile of Williams syndrome: a complex pattern of strengths and weaknesses. J Cogn Neurosci 2000; 12 (Suppl 1): 7–29.

Bellugi U, Lichtenberger L, Mills D, Galaburda A, Korenberg JR. Bridging cognition, the brain and molecular genetics: evidence from Williams syndrome. Trends Neurosci 1999; 22: 197–207.

Bellugi U, Marks S, Bihrle A, Sabo H. Dissociation between language and cognitive functions in Williams Syndrome. In: Bishop D, Mogford K, editors. Language development in exceptional circumstances. Edinburgh: Churchill Livingstone; 1988. p. 177–89.

Bellugi U, Wang PP, Jernigan TL. Williams syndrome: an unusual neuropsychological profile. In: Broman SH, Grafman J, editors. Atypical cognitive deficits in developmental disorders: implications for brain function. Hillsdale, NJ: Erlbaum; 1994.

Birch EE, Stager DR. Monocular acuity and stereopsis in infantile esotropia. Invest Ophthalmol Vis Sci 1985; 26: 1624–30.

Braddick OJ, O'Brien JM, Wattam-Bell J, Atkinson J, Turner R. Form and motion coherence activate independent, but not dorsal/ventral segregated, networks in the human brain. Curr Biol 2000; 10: 731–4.

Brefczynski JA, DeYoe EA. A physiological correlate of the 'spotlight' of visual attention. Nat Neurosci 1999; 2: 370–4.

Brodmann KK. Vergleichende Lokalisationslehre der Grosshirnrinde in ihren Prinzipien dargestellt auf Grund des Zellenbaues. Leipzig, Germany: Barth-Verlag; 1909.

Brunk HD. Introduction to mathematical statistics 363. New York, NY: Blaisdell Publishing Co.; 1965.

Castelo-Branco M, Mendes M, Sebastiao AR, Reis A, Soares M, Saraiva J, et al. Visual phenotype in Williams-Beuren syndrome challenges magnocellular theories explaining human neurodevelopmental visual cortical disorders. J Clin Invest 2007; 117: 3720–9.

Conner IP, Sharma S, Lemieux SK, Mendola JD. Retinotopic organization in children measured with fMRI. J Vis 2004; 4: 509–23.

Cox RW. AFNI: software for analysis and visualization of functional magnetic resonance neuroimages. Comput Biomed Res 1996; 29: 162–73.

Dale AM, Fischl B, Sereno MI. Cortical surface-based analysis. I. Segmentation and surface reconstruction. Neuroimage 1999; 9: 179–94.

DeYoe EA, Carman GJ, Bandettini P, Glickman S, Wieser J, Cox R, et al. Mapping striate and extrastriate visual areas in human cerebral cortex. Proc Natl Acad Sci USA 1996; 93: 2382–6.

Dougherty RF, Koch VM, Brewer AA, Fischer B, Modersitzki J, Wandell BA. Visual field representations and locations of visual areas V1/2/3 in human visual cortex. J Vis 2003; 3: 586–98.

Eckert MA, Tenforde A, Galaburda AM, Bellugi U, Korenberg JR, Mills D, et al. To modulate or not to modulate: differing results in uniquely shaped Williams syndrome brains. Neuroimage 2006; 32: 1001–7.

Engel SA, Rumelhart DE, Wandell BA, Lee AT, Glover GH, Chichilnisky EJ, et al. fMRI of human visual cortex. Nature 1994; 369: 525.

Farran EK. Orientation coding: a specific deficit in Williams syndrome? Dev Neuropsychol 2006; 29: 397–414.

Fischl B, Sereno MI, Dale AM. Cortical surface-based analysis. II: Inflation, flattening, and a surface-based coordinate system. Neuroimage 1999a; 9: 195–207.

Fischl B, Sereno MI, Tootell RB, Dale AM. High-resolution intersubject averaging and a coordinate system for the cortical surface. Hum Brain Mapp 1999b; 8: 272–84.

Frangiskakis JM, Ewart AK, Morris CA, Mervis CB, Bertrand J, Robinson BF, et al. LIM-kinase1 hemizygosity implicated in impaired visuospatial constructive cognition. Cell 1996; 86: 59–69.

Friston KJ, Ashburner J, Frith C, Poline J, Heather J, Frackowiak R. Spatial registration and normalization of images. Hum Brain Mapp 1995; 3: 165–89.

Galaburda AM, Holinger DP, Bellugi U, Sherman GF. Williams syndrome: neuronal size and neuronal-packing density in primary visual cortex. Arch Neurol 2002; 59: 1461–7.

Hasnain MK, Fox PT, Woldorff MG. Intersubject variability of functional areas in the human visual cortex. Hum Brain Mapp 1998; 6: 301–15.

Haxby JV, Grady CL, Horwitz B, Ungerleider LG, Mishkin M, Carson RE, et al. Dissociation of object and spatial visual processing pathways in human extrastriate cortex. Proc Natl Acad Sci USA 1991; 88: 1621–5.

Jenkinson M, Bannister P, Brady M, Smith S. Improved optimization for the robust and accurate linear registration and motion correction of brain images. Neuroimage 2002; 17: 825–41.

Kastner S, Pinsk MA, De Weerd P, Desimone R, Ungerleider LG. Increased activity in human visual cortex during directed attention in the absence of visual stimulation. Neuron 1999; 22: 751–61.

Kippenhan JS, Olsen RK, Mervis CB, Morris CA, Kohn P, Meyer-Lindenberg A, et al. Genetic contributions to human gyrification: sulcal morphometry in Williams syndrome. J Neurosci 2005; 25: 7840–6.

Landau B, Hoffman JE, Kurz N. Object recognition with severe spatial deficits in Williams syndrome: sparing and breakdown. Cognition 2006; 100: 483–510.

Lowel S, Singer W. Selection of intrinsic horizontal connections in the visual cortex by correlated neuronal activity. Science 1992; 255: 209–12.

Mervis CB, Morris CA. Williams Syndrome. In: Mazzocco MMM, Ross JL, editors. Neurogenetic developmental disorders: variation of manifestation in childhood. Cambridge, MA, US: The MIT Press; 2007. p. 199–262.

Mervis CB, Morris CA, Bertrand J, Robinson BF. Williams syndrome: Findings from an integrated program of research. In: Tager-Flusberg H, editor. Cambridge, MA: MIT Press, 1999.

Mervis CB, Robinson BF, Bertrand J, Morris CA, Klein-Tasman BP, Armstrong SC. The Williams syndrome cognitive profile. Brain Cogn 2000; 44: 604–28.

Meyer-Lindenberg A, Kohn P, Mervis CB, Kippenhan JS, Olsen RK, Morris CA, et al. Neural basis of genetically determined visuospatial construction deficit in Williams syndrome. Neuron 2004; 43: 623–31.

Meyer-Lindenberg A, Mervis CB, Berman KF. Neural mechanisms in Williams syndrome: a unique window to genetic influences on cognition and behaviour. Nat Rev Neurosci 2006; 7: 380–93.

Mobbs D, Eckert MA, Menon V, Mills D, Korenberg J, Galaburda AM, et al. Reduced parietal and visual cortical activation during global processing in Williams syndrome. Dev Med Child Neurol 2007; 49: 433–8.

Mobbs D, Garrett AS, Menon V, Rose FE, Bellugi U, Reiss AL. Anomalous brain activation during face and gaze processing in Williams syndrome. Neurology 2004; 62: 2070–6.

Morris CA, Mervis CB. Williams syndrome. In: Goldstein S, Reynolds CR, editors. New York, NY: Guilford Press; 1999.

Paul BM, Stiles J, Passarotti A, Bavar N, Bellugi U. Face and place processing in Williams syndrome: evidence for a dorsal-ventral dissociation. Neuroreport 2002; 13: 1115–9.

Reiss AL, Eckert MA, Rose FE, Karchemskiy A, Kesler S, Chang M, et al. An experiment of nature: brain anatomy parallels cognition and behavior in Williams syndrome. J Neurosci 2004; 24: 5009–15.

Reiss AL, Eliez S, Schmitt JE, Straus E, Lai Z, Jones W, et al. IV. Neuroanatomy of Williams syndrome: a high-resolution MRI study. J Cogn Neurosci 2000; 12 (Suppl 1): 65–73.

Saad ZS, Chen G, Reynolds RC, Christidis PP, Hammett KR, Bellgowan PS, et al. Functional imaging analysis contest (FIAC) analysis according to AFNI and SUMA. Hum Brain Mapp 2006; 27: 417–24.

Schmitt JE, Eliez S, Bellugi U, Reiss AL. Analysis of cerebral shape in Williams syndrome. Arch Neurol 2001; 58: 283–7.

Sereno MI, Dale AM, Reppas JB, Kwong KK, Belliveau JW, Brady TJ, et al. Borders of multiple visual areas in humans revealed by functional magnetic resonance imaging. Science 1995; 268: 889–93.

Smith SM. Fast robust automated brain extraction. Hum Brain Mapp 2002; 17: 143–55.

Somers DC, Dale AM, Seiffert AE, Tootell RB. Functional MRI reveals spatially specific attentional modulation in human primary visual cortex. Proc Natl Acad Sci USA 1999; 96: 1663–8.

Thompson PM, Lee AD, Dutton RA, Geaga JA, Hayashi KM, Eckert MA, et al. Abnormal cortical complexity and thickness profiles mapped in Williams syndrome. J Neurosci 2005; 25: 4146–58.

Tychsen L, Wong AM, Burkhalter A. Paucity of horizontal connections for binocular vision in V1 of naturally strabismic macaques: Cytochrome oxidase compartment specificity. J Comp Neurol 2004; 474: 261–75.

Ungerleider LG, Mishkin M. Two cortical visual systems. In: Ingle J, Goodale MA, Mansfield RJW, editors. Analysis of visual behavior. Cambridge, MA: MIT Press; 1982. p. 549–86.

Van Essen DC. Surface-based approaches to spatial localization and registration in primate cerebral cortex. Neuroimage 2004; 23 (Suppl 1): S97–107.

Van Essen DC, Dierker D, Snyder AZ, Raichle ME, Reiss AL, Korenberg J. Symmetry of cortical folding abnormalities in Williams syndrome revealed by surface-based analyses. J Neurosci 2006; 26: 5470–83.

Vicari S, Carlesimo GA. Short-term memory deficits are not uniform in Down and Williams syndromes. Neuropsychol Rev 2006; 16: 87–94.

Watanabe K, Shimojo S. Attentional modulation in perception of visual motion events. Perception 1998; 27: 1041–54.

Wechsler D. Manual for the Wechsler Adult Intelligence Scale-Revised (WAIS-R). San Antonio, TX: The Psychological Corporation; 1981.

Wechsler D. Wechsler Abbreviated Scale of Intelligence. San Antonio, TX: The Psychological Corporation; 1999.

Wohlschlager AM, Specht K, Lie C, Mohlberg H, Wohlschlager A, Bente K, et al. Linking retinotopic fMRI mapping and anatomical probability maps of human occipital areas V1 and V2. Neuroimage 2005; 26: 73–82.